GREENER AVIATION 2016
SQUARE MEETING CENTRE, BRUSSELS, BELGIUM / 11–13 OCTOBER 2016

Simulation of an electro-mechanical ice protection system for aircraft structure based on ultrasonic guided wave

Hossein Habibi[(1)], Alvin Yung Boon Chong[(1), (*)], Jamil Kanfoud[(1)], Cem Selcuk[(1)], Tat-Hean Gan[(1)] and Dominique Mayhew[(2)]

[(1)] Brunel Innovation Centre (Brunel University London), Granta Park, Great Abington, Cambridge, CB21 6AL United Kingdom. Phone: +44 (0)1223 899512; Email: bic@brunel.ac.uk
[(2)] Safran Aircraft Engines, Rond-point René Ravaud – Réau, 77550 Moissy-Cramayel, France Email: dominique.mayhew@safrangroup.com
[(*)] Speaker

KEYWORDS: Ultrasonic guided wave, ice protection system, carbon-fibre-reinforced polymer, finite element method, open rotor propeller, aerospace.

ABSTRACT:

The benefits of greater fuel savings and lesser environmental effects (i.e. better efficiency and lower emission) through the use of avant-garde open rotor propeller unfolded the next technology for the imminent generation of single-aisle aircraft. However, ice accretion on aircraft during in-flight significantly affects the aerodynamic performance and control of the plane due to the increment of drag and imbalance caused by the non-uniform mass of ice. This continues to be a concern as it is widely known to be causing safety incidents. Thus, in order for the open rotor propeller technology to take forward with improved aviation safety, method must be found to enable power efficient de-icing system in particular targeting the leading edge of the open rotor blade which is prone to ice accretion. In this paper, we investigate the use of an electro-mechanical technique involving piezoelectric actuators to excite shear stresses on the Carbon-Fibre-Reinforced Polymer (CFRP) blade structure which potentially led to the de-bonding of ice from the surface. Essentially, this Ultrasonic Guided Wave (UGW) Ice Protection System (IPS) is subject to Finite Element Method (FEM) analysis to study the wave propagation through the CFRP blade and ice configurations. The optimum excitation of the actuator is then determined by the generated shear stress which exceeds the adhesive shear strength for ice and composite. The developed computational model of UGW based IPS allows the excitation parameters to be optimised for de-icing of various ice conditions. The optimum parameters will form the basis of instrumentation for the experimental trial to be underway.

1. INTRODUCTION

Ice accretion during flight of an aircraft affects the performance and control of the plane. The earliest Icing Protection Systems (IPS) were investigated and implemented to fixed wing aircraft between 1935 and 1949 [1]. Since the introduction of Carbon-Fibre-Reinforced Polymer (CFRP) material in the industry, this has become increasingly popular in aviation applications such as the aircraft open rotor propeller, fuselage and aileron. It is highly due to the superior properties (i.e. corrosion resistance, improved fatigue performance, high specific strength to weight ratio). However, aircraft icing remains to be a concern since it has caused 583 civil aviation accidents and over 800 fatalities in the U.S. alone between 1982 and 2000 [2]. The altitude range of operation of single-aisle aircraft makes them susceptible to encounter icing conditions. In addition, economic pressures dictate that aircraft must keep flying in known adverse weather conditions and these pressures will continue to increase. Moreover, there will always be risks that a flight will run into unpredictable icy forming conditions even when departing in good weather.

On open rotor propeller aircraft, the leading edge of the propeller blade has been identified to be

vulnerable to ice accretion in flight, as well as on the ground. Propeller blades operating at temperatures below -10ºC tend to collect ice along the majority of the blade's leading edge [3]. Water can freeze on impact with the leading edge of the rotor blade when a combination of temperatures close to freezing, high wind speeds, and high cloud water concentrations occur [4]. The increased mass manifest the drag and consequently decreases lift. The ice accretion also caused unevenly distribution of weight which prejudices the flight equilibrium which is hazardous. Ice also causes the control and propulsion mechanisms to be reduced in efficiency and even seize up which consequently endanger the aircraft. In addition, ice can also be dangerous on propellers and rotors because these structures are finely balanced and any moderate ice accretion can seriously affect the balance, causing stress or vibration levels which could threaten structural integrity [5 - 9].

There are various active ice protection systems for aircraft such as electro-Impulse, electro-expulsive separation systems, hot-air, electrical heating [10]. The thermal systems require large power consumption, the mechanical system have limited efficiency. In this paper, the study focuses on the use of guided waves excited into blade material utilizing ultrasonic transducers at appropriate frequencies. In this regards, there are two major issues to be resolved. First, ensuring guided wave to propagate in the blade structure and secondly is to generate sufficient shear stress in the ice-blade interface for breaking off ice bond. The effects of wave propagation in plates of regular shapes have been well studied in literature [11, 12]. On the contrary, guided waves with regards to propeller blades of complex geometry especially for ice protection applications under severe weather conditions have not been of full interest yet and it needs fundamental investigation. In this study, potential location for mounting transducer and wave excitation will be examined. To carry out the analyses, commercial Finite Element Method (FEM) software namely COMSOL® Multiphysics 4.4 (COMSOL) has been used.

- To investigate propagation of guided waves in blade structure and calculate stress distribution and energy concentration on the critical areas of the blade prone to icing.
- To specify optimal exciting frequency and other signal characteristics to achieve efficient performance for anti-icing and de-icing. This selection is mainly accomplished numerically through dispersion curves and the concept of Interfacial Stress Concentration Coefficients (ISCC) [13].
- To determine possible location for installing transducer at which (i) the largest possible area of the critical iced area including leading edge is covered (ii) the transducer is easily installable and maintainable (iii) loss of blade material is minimised.
- To characterise the best direction of excitation for transducer to transmit efficient energy to the leading edge of the blade for best de-icing performance.

The strategy of ultrasonic guided waves as a technique for ice protection is based on generation of sufficient shear stress at the ice/substrate interface through choosing optimal wave modes and frequencies to break the adhesive bond between the blade substrate and the accreted ice. The required stress for de-icing performance depending on physical properties of both homogeneous blade material and type of ice has been reported from 0.02 to 1.66 MPa. In literature [14, 15], it shows shear adhesion strength between aluminium and two types of ice. Reference [15] has specified the adhesive strength of ice formed on a composite blade of helicopter as maximum 0.4 MPa which is the most related case to our study. So this amount of stress has been considered as a basic criterion through this work to de-bond the ice accreted on the blade surface. The challenge is how to propagate waves appropriately and subsequently generate interface shear stress to exceed the adhesion strength between the ice and the blade surface, while reducing the in-plane shear stresses simultaneously in order not to cause any damage to the blade itself. This has led to utilising ISCC concept for compromising between these two levels of stress which will be discussed.

To address the objectives, this paper describes the approach of numerical FEM modelling and its related theories and algorithms in the following section. Then the benchmark model details and some other properties and considerations in FEM simulation will be explained. It will be followed by the section demonstrating dispersion curves and Interfacial Stress Concentration Coefficients (ISCC) calculated for blade model to select wave mode and central frequency. Then the optimised wave characterize will be subjected to numerical modelling based on transient analysis using externally mounted transducer will be presented.

2. FREQUENCY ANALYSIS APPROACH

Figure 1 show the modelling procedure followed in this study. This FEM commercial package is operated on the basis of numerical solutions of Partial Differential Equations (PDEs) built up for working out the system response. Using Structural Mechanics module of COMSOL via eigenfrequency function, initial data for dispersion curve and ISCC analyses will be obtained. Then the dispersion curves according to the approaches can be achieved [11, 12]. The swiping frequency can be covered up to hundreds of kilohertz. Based on the curves specifications, appropriate frequency will be selected in order to concentrate power at the leading edge of the blade. Subsequently stress and displacement distribution upon the critical iced area of the blade are simulated and displayed to check if (i) the wave can propagate in the blade in proper direction, (ii) the generated shear stress at interface is sufficiently high to de-bond the ice layer.

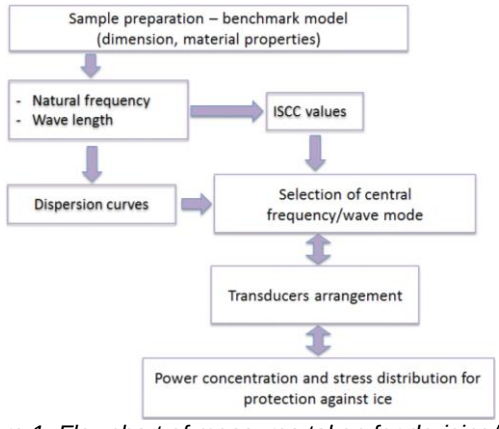

Figure 1. Flowchart of measures taken for de-icing/anti-icing the propeller blade in modelling phase.

The FEM package through solving PDEs offers a numerical technique to find mode shapes and approximate values of resonance frequencies which makes it possible to derive dispersion curves and predict the dynamical behaviour and dispersive properties of the structure. Such FEM software breaks down complex structures into connected nodes in the form of a grid known as mesh. This mesh which consists of elements contains all the properties of the model defined by structural parameters. The modal analysis in the current case is represented by generalized Equation [16],

$$f = \frac{Imag(\lambda_{eigen})}{2\pi} \qquad (1)$$

which are specified and applied to every node in the mesh. λ_{eigen} is associated with the eigenvalue. In frequency-based analyses, the finer the mesh size, the more accurate the results will be. However, higher mesh densities leads to increase calculations rapidly. For this reason, a trade-off should be made to compromise between computational time and the accuracy of modelling results.

It is possible to obtain the maximum mesh element size in which each peak and trough in vibration can be surely measured. To do this, the wave speed must be the maximum value for the slowest wave mode in the operating range. Acoustic wave propagate through a material in the same form of a mechanical stress wave meaning that they travel at the speed of sound in that medium. The spacing between mesh elements can be figured out by substituting the speed of sound for that medium in Equation 2.

$$\lambda_{min} = \frac{c}{F_s} \qquad (2)$$

where λ_{min} is the minimum distance between mesh elements and F_s stands for the sampling frequency. The minimum number of elements recommended for a wavelength to achieve best results, based on a convergence study, is 10 [16]. Therefore the maximum element size to be used for defining mesh size yields.

$$\max. element\ size = \frac{\lambda_{min}}{10} \qquad (3)$$

The geometrical details of the CFRP blade are depicted in Figure 2. The blade is about 1.2 m long with a chord of 0.5 m long at the root and 0.2 m long at the tip. Leading edge and trailing edge of the blade have been both considered rectilinear with no curvature. A view of the blade's cross section at root is also shown in Figure 2. The critical zone subject to icing has been also pointed in Figure 2. This critical area including 20% of the chord and 60% of the span length at the leading edge is the area which must be protected against icing as extensively as possible.

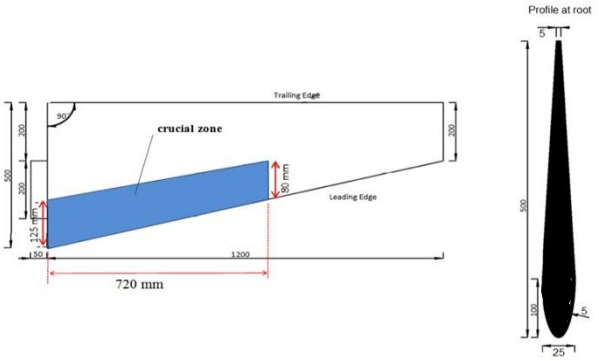

Figure 2. Representation of the benchmark model of CFRP propeller blade in which the critical iced zone is highlighted in blue; the cross section profile of the blade is shown on the right (Dimensions in mm).

The blade root is attached to the hub of the propeller rotor. In other words, the root connects the blade to the hub of propeller so that the blade is considered as clamped at its boundary edge with all its six degrees of freedom constrained. The mechanical properties of both blade material and the formed glaze ice in this simulation are given in Table 1. The characters E, ρ and v refer to Young's modulus, density and Poisson's ratio respectively.

Material	E=Young's Modulus (GPa)	v=Poisson's Ratio	ρ=Density (kg/m^3)
CFRP	46.2	0.337	1575
Ice	0.351	0.351	917

Table 1. Input material properties.

A 2-mm ice layer on the blade embracing the area of interest is considered in the model. Figure 3 illustrates a 3-D representation of the generated FE model including the formed ice layer.

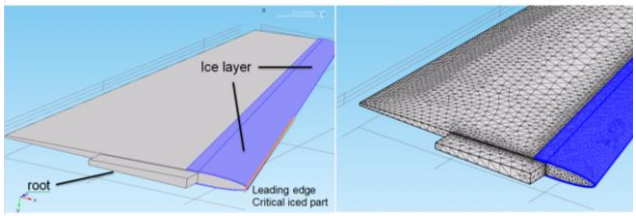

Figure 3. The FEM, 3-D model of the propeller blade and formed ice layer.

Altogether, the entire model was built up using 278565 tetrahedral elements (domain, boundary and edge) with an increased congestion in the edges or the lines at which the slope of surfaces change abruptly. By modelling the complex vibration modes present in the blade model, it was possible to derive a dispersion curve and predict the dispersive properties of the blade structure to a reasonable level of accuracy. This was performed using eigenfrequency followed by post-processing through MATLAB coding. Two critical parameters are still required in order to plot a dispersion curve namely phase velocity and wavelength [11]. Wavelength can be determined by observing the mode shape for each eigenfrequency. Wavelength defines the distance travelled by a complete wave, and can therefore be calculated using the following equation.

$$\lambda = \frac{L}{n} \tag{4}$$

where L is the length of the geometry being modelled (e.g. leading edge of the blade) and n is the number of complete cycles observed from the mode shape.

The number of cycles is calculated from the shape of the variation along the leading edge of the blade. The data extracted here were post-processed using a code which loaded and plotted the total displacement variation data, and counted the number of peaks and troughs for each wave mode for the entire eigenfrequencies. Using this information, the number of cycles was calculated using the following formula:

$$n = \frac{N_{of}peaks + N_{of}troughs}{2} \tag{5}$$

Once the number of cycles was calculated, the wave length for that mode was also calculated, and a phase velocity dispersion curve was generated. Also the Interface Stress Concentration Coefficient (ISCC) is defined by the following equation when the x-axis is the direction of wave propagation,

$$ISCC = \frac{\sigma_{yz}|_{layer\ interface}}{\sqrt{power}} \tag{6}$$

Here σ_{yz} is the stress tensor component at the interface between sample and ice, and power is defined by the following equation when z is the direction along thickness.

$$power = \int_{thickness} P_x dz \tag{7}$$

where P is the Poynting's vector defining the power flow on the structure and $P = [P_x, P_y, P_z]$. The governing equation for parameter P is shown in Equation 8:

$$P = \frac{-\vec{v}^* \cdot \sigma}{2} \qquad (8)$$

where $\vec{v}$ is particle velocity, * is the complex conjugate and σ is the stress tensor.

In COMSOL, shear stress can be obtained directly by the parameter 'Stress tensor (Spatial), Stress tensor, (yz or xz or yz) component (soild.syz)' and P can be calculated using integral function against the thickness of Complex mechanical energy flux, X (or Y or Z) component (W/m). Therefore, ISCC can be calculated according to Equation 6. The ISCC provides the criteria for selecting the central frequency and wave mode for ultrasonic de-ice are: (i) The larger the ISCC, the less power would be required for the de-icing system to be effective, (ii) the central frequency and wave mode should be non-dispersive in dispersion curves.

3. EIGENFREQUENCY ANALYSIS RESULTS

The dispersion curve and ISCC for the composite blade with 2-mm ice layer, based on shear stress S_{xy}, are calculated and shown in Figure 4a-b. This yields the optimised central frequency, phase velocity and wave length of ultrasonic wave chosen as 53.65 kHz, 2949 m/s and 0.0549 m respectively. Note that once frequency and wave mode are chosen, the phase velocity can be worked out as a dependent parameter. For convenience in selecting the optimum wave mode and central frequency, Figure 4c represents superimposition of dispersion curves and ISCC values in one combined plot.

Figure 5, as another example, shows dispersion curves, ISCC values and the combination of them based on the highest ISCC values that are attainable when the shear stress S_{yz} is considered as the criteria. Likewise, similar calculations were carried out on the basis of the shear stress S_{xz} to find the optimum range of central frequency and wave modes. The summary of results for these three shear stresses has been listed in Table 2.

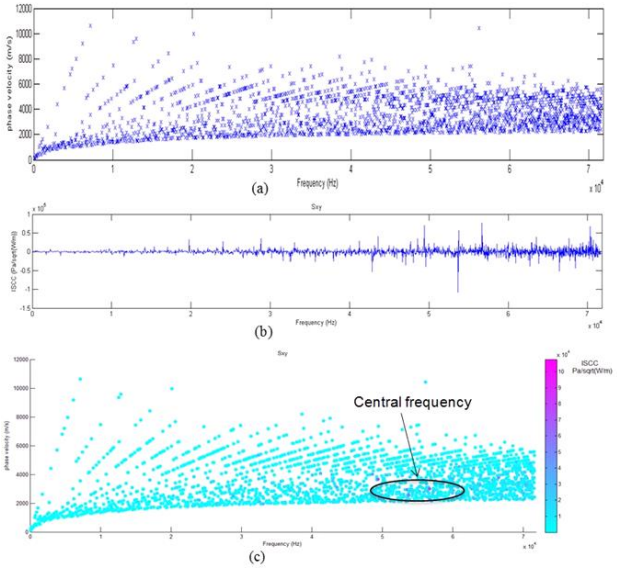

Figure 4. (a) Dispersion curve, (b) ISCC graph, (c) Combination of dispersion curve and ISCC values; for the blade with 2 mm ice layer to find non-dispersive modes of high ISCC based on S_{xy} which has been indicated by an oval shape.

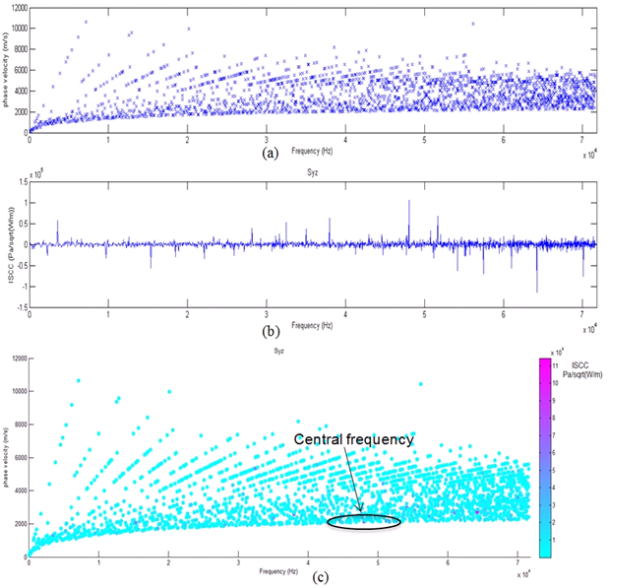

Figure 5. a) Dispersion curve, b) ISCC graph, c) Combination of dispersion curves and ISCC values; for the blade with 2 mm ice layer to find non-dispersive modes of high ISCC based on S_{yz} which has been specified by an oval shape.

Optimised wave parameters (blade + 2mm ice) / Criteria	fc (kHz)	Phase velocity (m/s)	Wave length (m)
S_{xy}	53648	2949	0.0549
S_{xz}	32472	5355	0.1649
S_{yz}	48028	2160	0.0449

Table 2. Summary of simulation results on selection of central frequency, phase velocity and wave length using three different shear stresses as criteria.

4. TRANSIENT ANALYSIS APPROACH

In addition, time dependent analysis was utilised to investigate the transient power and stress distribution and ultrasound wave propagation generated by a transducer array. The following model approach is based on the time-dependant equation obtained from Newton's second law [16].

$$\rho \frac{\partial^2 \boldsymbol{u}}{\partial t^2} = \nabla . s + \boldsymbol{F}v \qquad (9)$$

where u is the displacement vector due to the elastic effect, s is the stress tensor and $\boldsymbol{F}v$ represents the volume force vector. The excitation frequency will follow the values for different criteria; the time period for simulation is depending on phase velocity and the distance between ultrasonic transducers with respect to wave length. In this section, the shear waves using criteria S_{yz}, as a first attempt, listed in Table 2 is excited and propagated through the solid blade especially along the critical areas prone to icing (i.e. the leading edge). The primary factor is the central frequency at which transducers should be excited based on ISCC defined by Equation 6, a shear stress value at the interface of ice/ blade substrate has to be maximised. In each structure, depending on geometry, shape, composite fibre orientations or type of ice, it is worth to note that one of the shear stresses could be more effective in breaking the ice bond.

A sinusoidal signal of 5 cycles applying the pressure amplitude 5×10^6 N/m^2, as schematically shown in Figure 6, was used for transducers to excite ultrasonic waves in the blade. The time interval of signal cycles has been chosen with respect to the phase velocity of the wave given in Table 2 and the critical length of the blade (0.72 m). The time period of the signal is determined such that if too long (i.e. more than one millisecond), it is likely that the shear wave is intervened by wave reflections from the blade geometrical boundaries before the generated shear stress for de-bonding the ice at interface comes into effect. In other words, the shear wave becomes inefficient due to waves interference and interruption of original launched wave and consequently increase attenuations and losing power focus on the area of interest. On the other hand, if the signal is too short (i.e. < 0.1 ms), then the time taking for ice protection would be unnecessarily increased which might leads to an uneven coverage across the critical area within a same time domain.

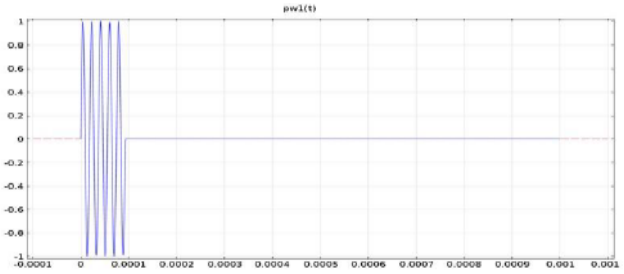

Figure 6. Sinusoidal signal transmitted by ultrasonic transducers to propagate wave in the blade.

It should be noted that only small area of the blade surface is prone to be used for installing the transducer. Obviously it would be more efficient if transducer could be mounted somewhere close to the critical iced area which is at top surface of the blade. However any change or adding features on the external profile of blade might easily lead to malfunction or degradation of aerodynamic performance. Therefore the part remaining potential for mounting transducer is the bottom end of the leading edge near the blade root as circled in Figure 7. This area is also subjected to minimum dynamic forces applied to the blade and it apparently causes the least aerodynamic disturbance for blade. In addition, it also offer the following advantages,

i. The transducer does not need to be embedded during manufacturing of the blade.
ii. There is no need to spare any space inside the blade body for additional features.
iii. Repair and maintenance would be much more convenient in the case of any technical fault for the transducer.

The transducer material properties are modelled as Young's Modulus (129.22 GPa), Poisson Ratio (0.32) and density (7850 kg/m^3).

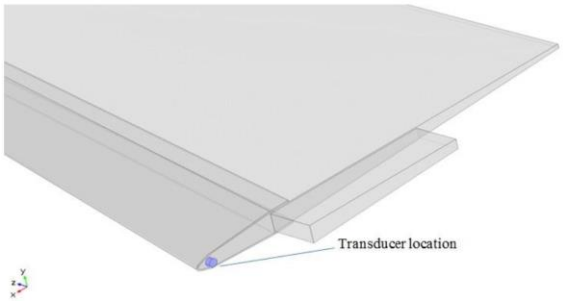

Figure 7. A single ultrasonic transducer placed outside the blade near to the root.

5. TRANSIENT ANALYSIS RESULTS

The transient distribution of stress is calculated using the central frequency and wave length of 48.03 kHz and λ=0.0449 m respectively (criteria Syz provided in Table 2). The time calculated range from 0 to 1 ms at 1 µs step. Figure 8 indicates that at time 0.265 ms the shear stress S_{yz} covering almost entire the critical iced zone at the interface which can reach to 1.5 MPa on average, which according to most criteria reported in the literature, is more than sufficient to de-bond the ice. The distribution of von Mises stress at different times at 0.215, 0.265 and 0.32 ms are shown in figure 9 to 11 respectively. According to these results, the ultrasonic wave was guided to propagate along the direction of interest and power was concentrated on the leading edge of the blade. Then it gradually spreads into the other areas of the blade.

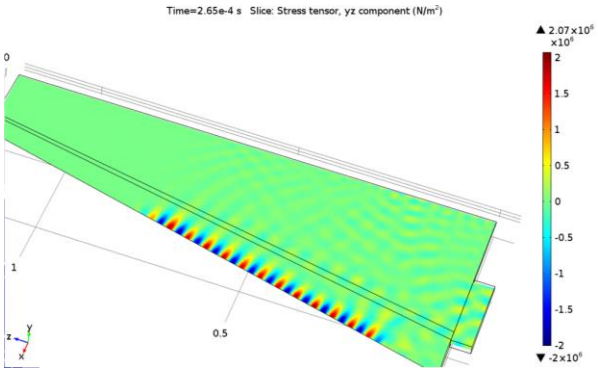

Figure 8. Distribution of the shear stress S_{yz} upon blade when transducer is excited at f = 48.03 kHz, in a transient state of wave propagation at t=0.265 ms.

Likewise, Figure 12 highlights symmetry of the wave on both sides of the blade surface at the same time as shown in Figure 9.

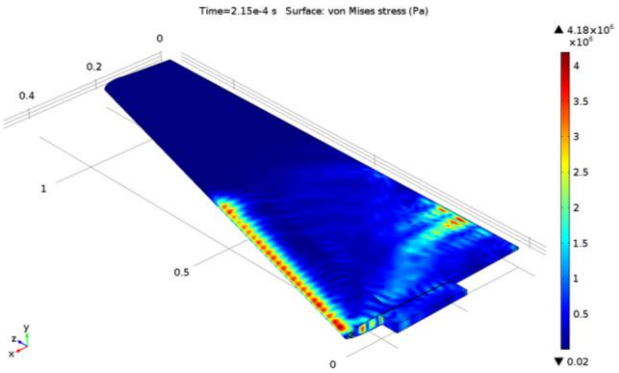

Figure 9. Distribution of von Mises stress upon blade when a single transducer placed outside the blade is excited with f=48.03 kHz at t=0.215 ms.

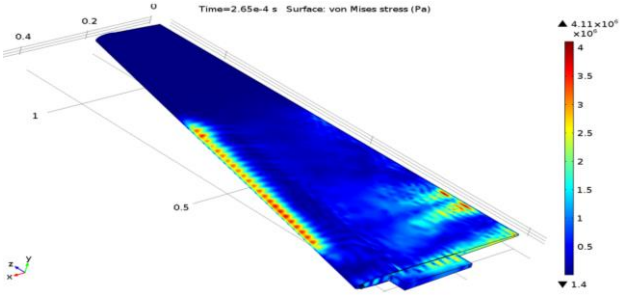

Figure 10. Distribution of von Mises stress upon blade when a single transducer placed outside the blade is excited with f=48.03 kHz at t=0.265 ms.

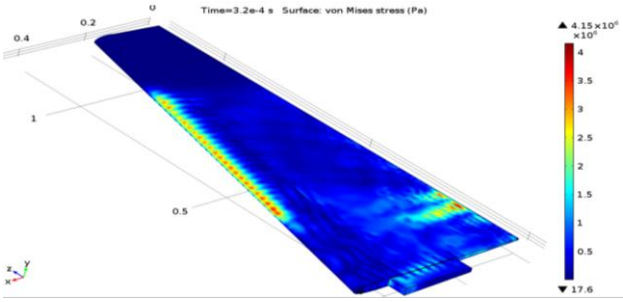

Figure 11. Distribution of von Mises stress upon blade when a single transducer placed outside the blade is excited with f=48.03 kHz at t=0.32 ms.

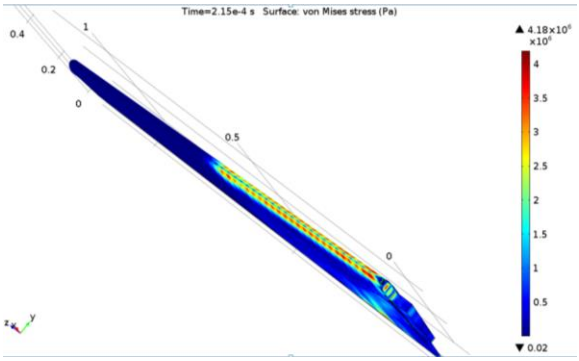

Figure 12. A different view of the blade showing surfaces on its both sides using the same characteristics described in Figure 9.

For more clarity on the variation of stress values, Figure 13 shows how the shear stress (S_{yz}) changes at the front line of the leading edge (ice/blade interface). Each graph represents one of the time steps in simulation. It is observed that sufficiently high values of stress (> 0.4 MPa) during a short time are generated at the most important part of the blade to be protected against icing. These results demonstrate the capability of a single transducer mounted outside the blade body which is minimal requirement in using ultrasonic guided waves for an ice protection system.

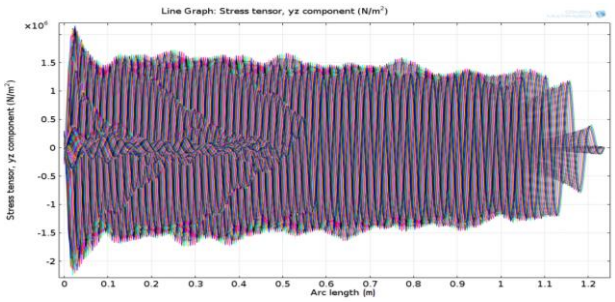

Figure 13. Variations of the shear stress S_{yz} over front line of the blade leading edge at different simulation time steps within 0.1 ms while a transducer mounted outside the blade excited at f=48.03kHz.

Finally, it should be noted that ultrasonic guided wave technique is likely to consider a low-consuming power compared to the thermal methods. Based on reference [13], it suggests the following equation for dissipative power consumption of material by an electro-mechanical actuator can be calculated in theory.

$$P_p = \frac{V^2 Re(Y)}{2} \qquad (10)$$

where V is the applied voltage and Y is the admittance of the system. In the current study, transducer input was defined as the force applying on the blade material. The power required for an actuator at a certain operational frequency can be estimated theoretically using ISCC definition given by Equation 6 in which depends on the shear stress generated at the ice interface and ISCC value. For instance, according to the results, the excited frequency of ca. 48 kHz is an optimum frequency to excite the blade. In Figure 5b, the blade leading edge at this frequency finds an ISCC value of 0.11 MPa/sqrt(W/m) which is substituted in Equation 6. Also the value of shear stress S_{yz} is needed which can be taken from modelling results. For example, the case shown in Figure 8 is considered; a maximum shear stress of 2 MPa is experienced by a point in the middle of leading edge. Substituting this value in Equation 10 yields pmax equal 0.33 kW/m^2 which is the maximum power needed for a single transducer placed at exterior of the blade operating at 48 kHz in one de-icing action. Albeit this is only a basic estimation from a mechanical point of view but it implies an approximate range of power to be considered as another characteristic in selecting appropriate transducers. It can also infer the efficiency of this technology compared to thermal methods.

6. CONCLUSION

This paper has described the feasibility of using an electro-mechanical de-icing system tailored for a representative open rotor propeller (i.e. benchmark model). It highlights the computational modelling approach based on eigenfrequency analysis coupled with the ISCC concept to yield the optimum excitation frequency (i.e. S_{yz} excitation at ca. 48 kHz). Subsequently the model is subjected to transient analysis in which the stress over the region of interest (i.e. leading edge of the blade) is obtained and results have shown to be promising in term of de-icing at low consuming power (shear stress exceeding the shear adhesion of ice-composite interface at 0.4 MPa). The basis of these preliminary studies will be extended to model the actual propeller blade design which will potentially involve further investigation of this technique such as using array of transducers which can practically mounted on the blade to enhance the guided wave energy for higher de-icing area coverage. It is worth noting that such transducers array strategy will inevitably scale up the power consumption of the system. Ultimately, the information obtained through these computational studies will be used to facilitate the development of the ultrasonic guided wave ice protection system leading to performing the actual experimental campaign at icing wind tunnel.

7. ACKNOWLEDGEMENTS

The research leading to these results has received funding from the European Community's **CLEANSKY Joint Technology Initiative for Aeronautics and Air Transport** managed by REA-Research Executive Agency, under grant agreement **JTI-CS-2013-1-SAGE-02-030**. The research has been undertaken as a part of the project entitled "Open rotor propellers Ice Protection System" – ICEPS-ORPS, in the collaboration between the following organizations: Brunel University London, TWI Limited and Safran Aircraft Engines. Project website: http://www.iceps-orps.eu/

8. REFERENCES

[1] Jackson, D. & Goldberg, J., (2007). Ice Detection Systems: A Historical Perspective. SAE International Conference, 2007-2007-01-3325, Seville, Spain.

[2] Petty, K.R. & Floyd, C.D.J., (2004). A Statistical Review of Aviation Airframe Icing Accidents in the U.S. 11th Conference on Aviation, Range, and Aerospace Meteorology. Massachusetts, United States of America.

[3] Coffman, H.J., (1987). Helicopter Rotor Icing Protection Methods. Journal of the American Helicopter Society, **32**(2), 34 – 39.

[4] Gent, R.W., Dart, N.P. & Candsdale, J.T., (2000). Aircraft Icing. Philosophical Transactions of the Royal Society of London Series A, **358**, 2873 – 2911.

[5] Ranaudo, R., Batterson, J., Reehorst, A., Bond, T. & O'Mara, T., (1991). Effects of Horizontal Tail Ice on Longitudinal Aerodynamic Derivatives. Journal of Aircraft, **28**, 193-199.

[6] Weisend, N. & Weisend Jr., (1989). Design of an Advanced Pneumatic Deicer for the composite rotor blades. Journal of Aircraft. **26**, 947-950.

[7] Scavuzzo, R., Chu, M. & Kellackey, C., (1991). Impact Ice Stresses in Rotating Airfoils. Journal of Aircraft, **28**, 450-455.

[8] Gurbacki, H.M. & Bragg, M.B., (2002). Unsteady Aerodynamic Measurements on an Iced Airfoil. 40th AIAA Aerospace Sciences Meeting. Nevada, United States of America.

[9] Bragg, M. B., Gregorek, G. M. & Lee, J.D., (1985). Aircraft Aerodynamics in Icing Conditions. Journal of Aircraft. **23**(1), 76-81.

[10] Goraj, Z., (2004). An overview of the deicing and antiicing technologies with prospects for the future. 24th International Congress Of The Aeronautical Sciences. Yokohama, Japan.

[11] Gómez, P., Fernández, J.P. & García, P.D., (2011). Lamb Waves and Dispersion Curves in Plates and its Applications in NDE Experiences Using Comsol Multiphysics. Stuttgart, Germany.

[12] Hora P., & Cervena, O., (2012). Determination of Lamb wave dispersion curves by means of Fourier transform. Journal of Applied and Computational Mechanics. **6**(1), 5–16.

[13] Zhu, Y., (2010). Structural tailoring and actuations studies for low power ultrasonic de-icing of aluminium and composite plates. *PhD Thesis*, College of Engineering, the Pennsylvania State University.

[14] Palacios, J., Smith, E., & Rose, J., (2011). Instantaneous Deicing of Freezer Ice via Ultrasonic Actuation, AIAA Journal, **49**(6), 1158-1167.

[15] Ramanathan S., (2005). Instantaneous Deicing of Freezer Ice via Ultrasonic Actuation. *PhD Thesis*, Engineering Science and Mechanics, the Pennsylvania State University.

[16] Comsol, Structural mechanics module user guide ver 4.4.